AIRCRAFT DESIGN USING A GRADIENT BASED OPTIMISATION TECHNIQUE

Per Weinerfelt
SAAB Aerosystems, Sweden

Keywords: *Aerodynamic shape optimization, adjoint technique, Euler calculations, aircraft design*

Abstract

The present paper describes aircraft design by means of the aerodynamic shape optimisation system **cadsos** at SAAB. It is a general optimisation system which can handle both geometrical and aerodynamic multi-point design under multi-constraints. The optimisation technique is based on gradient calculation using flow and adjoint flow computations.

In order to demonstrate the capability of the system, the optimisation of a supersonic commercial aircraft is described. The wing and the body geometry was optimized using totally 62 design variables. As a result of the optimisation a drag reduction, at constant lift and geometrical constraints, of 15.7% was obtained.

1 Introduction

An aerodynamic shape optimisation system, cadsos, has been developed at SAAB Aerospace during the last 5-10 years. The system has been extended and improved thanks to the work performed within to the European project AEROSHAPE. We will briefly describe the cadsos system and its application to aircraft design below. The system is using a gradient based optimisation technique. Gradients of the objective function or physical constraints, such as drag, lift or pitching moment, are computed from the solution to the Euler/Navier-Stokes and the adjoint Euler/Navier-Stokes equations. Since the gradient formulation only contains surface integrals over the solid wall surfaces it is easy to implement. By using the adjoint technique the cost of the gradient calculations is independent of the number of design variables. For each flow quantity involved in the optimisation problem, an adjoint equation has to be solved. The numerical solution of the Euler and its adjoint equations are computed using a finite volume discretisation on general structured multi block grids. Standard central difference approximation with second and fourth order artificial dissipation is used for the space derivatives. Multi grid technique and local time stepping are applied to speed up the convergence to steady state. The flow and adjoint solver is object oriented and the implementation is in C++ mixed with FORTRAN. C++ was chosen because of its flexibility, reusability, efficiency and availability, and also because it has features which makes it well suited for large projects. FORTRAN 77 was used for routines in which computational efficiency is crucial. The flow and the adjoint solver are parallelized using MPI. The optimizer is written in MATLAB because of its simplicity and its built in support for numerical computations.

Several options for the surface modifications are available. The modified surfaces can be parameterised using B-splines, sinusoidal bump functions, aero-functions etc. For wing optimisation parameters describing the camber and twist can also be used. A modified constraint steepest descent algorithm is used to drive the optimisation procedure towards the optimum.

The different parts such as the grid generator, the flow solver, adjoint solver and the optimizer are integrated into the system.

A finite difference technique for gradient calculations has also been introduced. This enables a comparison of the accuracy of adjoint gradients and finite difference gradients.

The cadsos system has been applied in several projects at SAAB and we will here briefly describe the work performed within the AEROSHAPE project. One of the tasks was focused on the optimisation of a complete SCT (supersonic commercial transport) aircraft.

2 Optimisation Technique and Geometry Parameterisation

The optimisation technique in the present paper is based on gradient calculations. We have used one of the gradient formulations described in [2] or [5]-[6]. This formulation is obtained using the continuous Euler and adjoint Euler equations and is expressed in terms of surfaces integrals over the surface to be optimized S. It has proven to be accurate and easy to implement. In [2] it is shown that the variation of an objective function or physical constraint F yields

$$\delta F \approx \iint_S G \delta x_k n_k \, dS \tag{1}$$

where $G = \dfrac{\partial}{\partial x_i}(\varphi_i + \psi^t w_H u_i)$, φ_i is a function associated to F, ψ the adjoint Euler solution, w_H the Euler solution and u_i the Cartesian velocity component i. We assume that the surface to be modified is parameterized according to

$$\delta x_k = \sum_j \sum_i c_{ijk} b_{ij}, \quad k = 1,2,3 \tag{2}$$

where c_{ijk} are coefficients and b_{ij} basis functions. The choice of basis functions is governed by the applications. Spline functions, describing the twist or camber line of a wing or the radial distribution of a cylindrical body, are examples. Inserting (2) into (1) results in

$$\delta F \approx \sum_j \sum_i c_{ijk} \iint_S G b_{ij} n_k \, dS \; = \; (c, g) \tag{3}$$

where the tensors c and g in (3) are defined by $(c)_{ijk} = c_{ijk}$ and $(g)_{ijk} = \iint_S G b_{ij} n_k \, dS$.

The original optimisation problem is nonlinear and has to be solved iteratively. In each iteration step the following linearisation can be performed

$$\begin{cases} \min\limits_c \left(c, g^0\right) \\ (c, g^m) = \Delta^m, \quad m = 1, \ldots, M \\ (c, h^n) = \Delta^n, \quad n = 1, \ldots, N \end{cases} \tag{4}$$

where g^0 is the gradient of the objective function, g^m the gradients of M physical constraints, h^n the gradients of N geometrical constraints and $\Delta^{m,n}$ deviations from the target values of the constraints. Upper and lower bounds on c can also be imposed in order to assure a bounded solution.

Our experience is that the solution to (4) might sometimes lead to too large deviations from the original geometry and hence an unphysical design. We have instead chosen a slightly modified optimisation approach

$$\begin{cases} \min\limits_c \dfrac{1}{2} \|c\|^2, \\ (c, g^0) = \Delta^0 \\ (c, g^m) = \Delta^m, \quad m = 1, \ldots, M \\ (c, h^n) = \Delta^n, \quad n = 1, \ldots, N \end{cases} \tag{5}$$

where Δ^0 is a user defined parameter determining the decrease of the objective function in each design step. The solution to equation (5) can be solved exactly since it is a quadratic optimisation problem with linear constraints. Introducing the Lagrangian function associated to (5) we get

$$\begin{aligned} L = \; & \frac{1}{2}\|c\|^2 + \lambda_0 \left(\left(c, g^0\right) - \Delta^0\right) + \\ & \lambda_m \left((c, g^m) - \Delta^m\right) + \lambda_n \left((c, h^n) - \Delta^n\right) \end{aligned} \tag{6}$$

A local saddle point to L is obtained by setting all derivatives to zero.

$$\begin{cases} \dfrac{\partial L}{\partial c_{ijk}} = c_{ijk} + \lambda_0 g^0_{ijk} + \lambda_m g^m_{ijk} + \lambda_n h^n_{ijk} = 0 \\ \dfrac{\partial L}{\partial \lambda_0} = (c, g^0) - \Delta^0 \\ \dfrac{\partial L}{\partial \lambda_m} = (c, g^m) - \Delta^m \\ \dfrac{\partial L}{\partial \lambda_n} = (c, h^n) - \Delta^n \end{cases} \tag{7}$$

The system (7) is linear and can be solved by standard Gauss elimination. When c is computed a new surface grid is created by adding the grid corrections, obtained from (2), to the actual surface grid. A new surface grid can alternatively be computed by first adding c to the parameters describing the surface followed by a remeshing of the surface.

3 Gradient Validation

A comparison, between gradients from formulation (1) and approximative gradients from finite difference approximations, has been done in order to verify the accuracy of the formula (1). The validation has included both 2D and 3D test problems and we will here focus on the 3D applications.

In the first test case the flow over the ONERA M6 wing, at inviscid flow conditions, is considered. The free stream Mach number is M_∞=0.84 and the angle of attack $\alpha = 3.31$. The computational mesh consists of a single block grid having 192x32x48 cells. The twist of the wing was modified by means of 11 B-spline functions. The gradients of the drag, lift and pitching moment were first computed by finite differences using forward differencing for different values of the disturbance parameter ε. Following values on ε were applied, $\varepsilon = 0.1, 0.01, 0.005$ and 0.001. As can be seen in figure (1)-(3) there are quite large differences between the computed gradients and it difficult in advance to predict the optimal value of ε. In all figures it can be observed that ε between 0.005 and 0.01 seems to give the best results. The values 0.1 and 0.001 both result in too large deviations from the others. The gradient computed by the adjoint technique shows good agree with the best finite difference gradients for both C_L and C_m whereas some descrepancies can be observed for C_D.

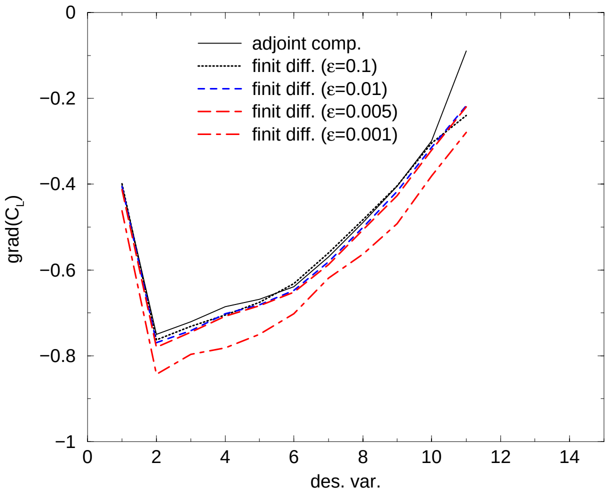

Fig. 1 Adjoint and finite difference gradient comparison of the lift of the ONERA M6 wing.

The second example is related to the optimisation of an SCT geometry at the inviscid flow condition M_∞=2.0 and C_L=0.12. Totally 62 design variables were used. The radial distribution and centre line of the body was controlled using 17 B-spline functions and the wing surface was modified by means of 45 B-spline functions describing the twist and the camber of the wing. For the finite difference calculations a disturbance parameter value of $\varepsilon = 0.005$ was applied. As can be seen in the figures (4) and (5) the agreement between gradients computed using adjoint versus finite difference technique is quite good.

4 Description of the SCT Geometry

The SCT aircraft configuration was first studied in the european project EUROSUP. A number of geometry modifications were introduced

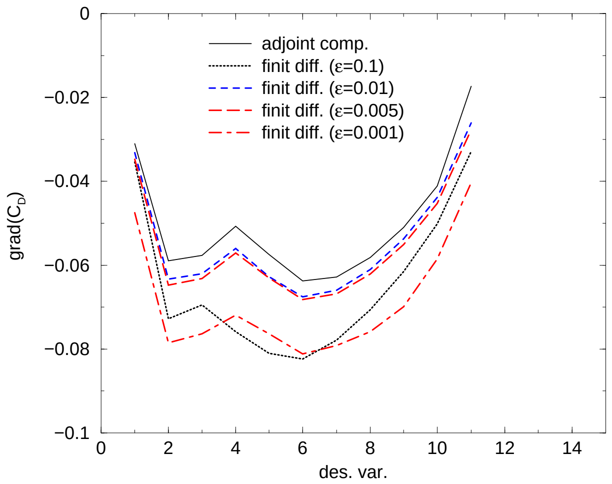

Fig. 2 Adjoint and finite difference gradient comparison of the drag of the ONERA M6 wing.

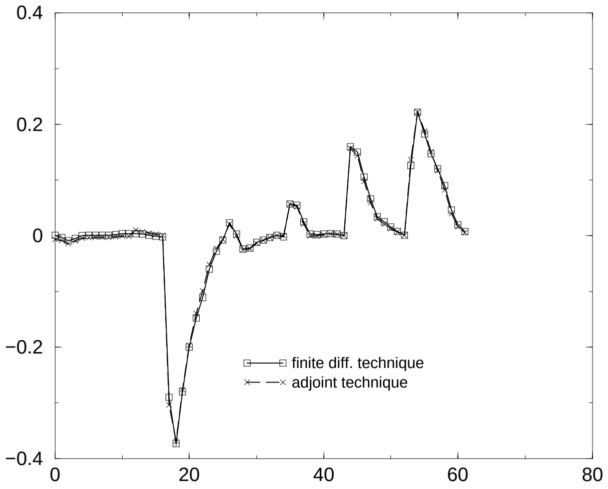

Fig. 4 Adjoint and finite difference gradient comparison of the lift of the SCT wing body geometry.

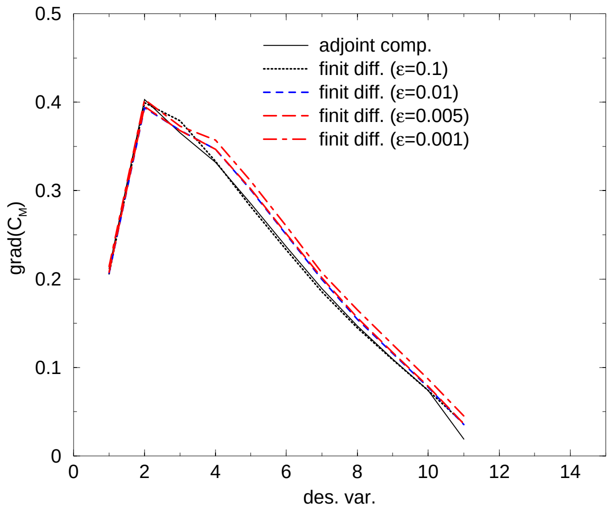

Fig. 3 Adjoint and finite difference gradient comparison of the pitching moment of the ONERA M6 wing.

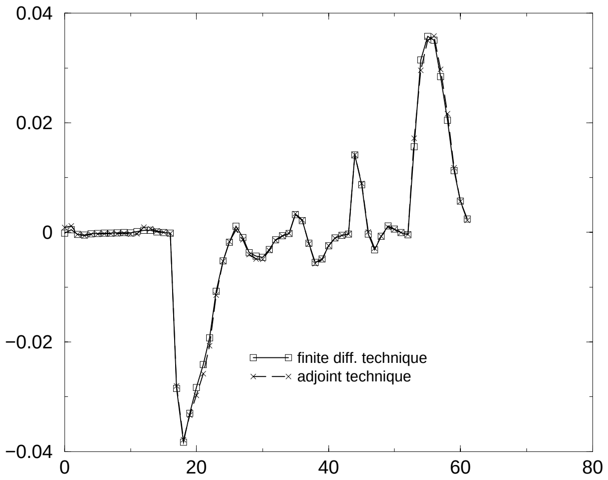

Fig. 5 Adjoint and finite difference gradient comparison of the drag of the SCT wing body geometry.

in order to ease CFD grid generation and analysis work. The modified baseline geometry was used as the starting point for the SCT optimisation study within AEROSHAPE (see e.g. [3] and [4]). The total fuselage length is 89 m and a constant cross sectional area is maintained over the fuselage centre section. The apex of the originally untwisted and uncambere wing is situated 21.374 m downstream of the fuselage. It has an inboard leading edge sweep angle of 71.5 degree and an outboard leading edge sweep angle of 51.5 degree. The wing span and the aspect ratio are 42 m and 2.11 m, respectively and the wing aerodynamic reference area is 840.87 m^2.

The baseline geometry of the EUROSUP wing/body configuration and the design criteria are described in detail in the technical document [1] of the EUROSUP research programme.

5 Surface and Volume Grid Generation

The CFD grid around the SCT geometry, applied in the present optimization study, consisted of 5 structured blocks and 196 000 cells. An executable version of the mesh generation system MEGACADS was provided by DLR in Braunscheig, Germany. It was coupled to the cadsos system at SAAB in order to perform the complete wing body optimisation. The mesh generation procedure was executed in batch mode by means of script files which were also developed at DLR. The multi block topology was kept fixed during the optimisation.

6 Results

It was agreed by all partners in AEROSHAPE, working on the STC optimization, to make use of the baseline geometry from the EUROSUP project and the design specifications in [1]. The objective function and constraints were also specified, according to the EUROSUP project. The initial block structured grid was generated by DLR [3] who also performed a grid feasibility study in order to provide an optimal setting of grid parameters such as the number of grid points, the grid density etc.

The aim of the SCT optimisation study was to demonstrate the capability of the enhanced optimisation methods, developed within AEROSHAPE, to handle many design parameters with acceptable costs. For this purpose simultaneous varations of both the fuselage and wing geometry was considered.

The optimization of the SCT geometry was performed at a free stream Mach number of M_∞=2.0 and C_L=0.12. The lift was treated as a constraint during the optimzation. A new surface and volume grid was generated by the MEGACADS system in each design step. The shape of the body was parameterized using 17 design variables, 12 for the radial distribution of the body in the stream wise direction and 5 for the body centerline. B-spline functions were applied as basis functions for the parameterisation. The wing was modified by means of a twist distribution spanned by 9 B-spline functions and 36 B-spline functions describing the camber at 9 span stations (i.e. 4 parameters for each station). The total degree of freedom for the complete wing body geometry was hence 62.

An adjoint based optimisation was first performed and the convergence history can be seen in figure 6 and 7. A drag reduction of 9.6%, at constant C_L, was obtained after 13 design cycles. The constraint on the lift was full filled without changing the angle of attack during the optimisation. The lift was hence fixed automatically by the values of the design parameters. There was no constraint on the pitching moment. In spite of that, the deviation of the pitching moment from the initial value was less than 3%.

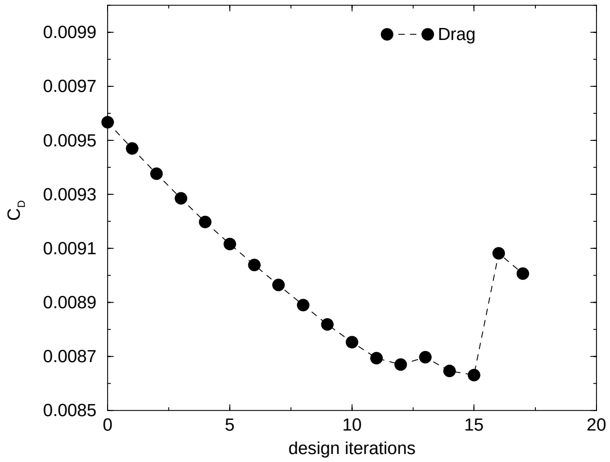

Fig. 6 SCT wing body optimisation convergence histories for drag.

A similar optimisation run, using finite difference gradients, was also performed. This resulted in a drag reduction of 9.5% after 15 design cycles.

As have been mentioned in section 3 the adjoint based gradients and the finite difference gradients agreed well. There are however some small differences for design variables 1-17 which corresponds to the parameterisation of the body.

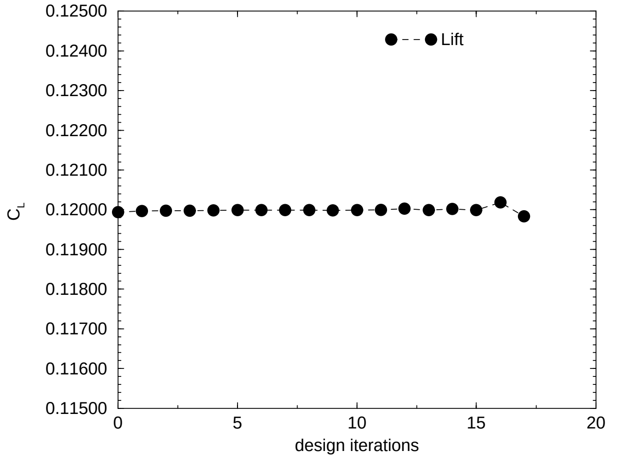

Fig. 7 SCT wing body optimisation convergence histories for lift.

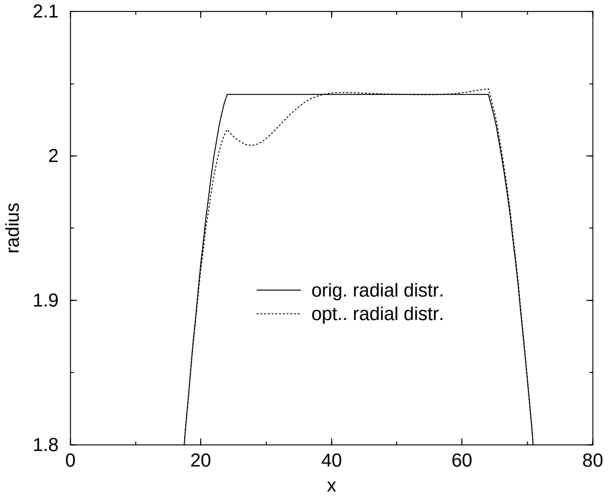

Fig. 8 SCT body radius distribution for the original and adjoint optimised configuration.

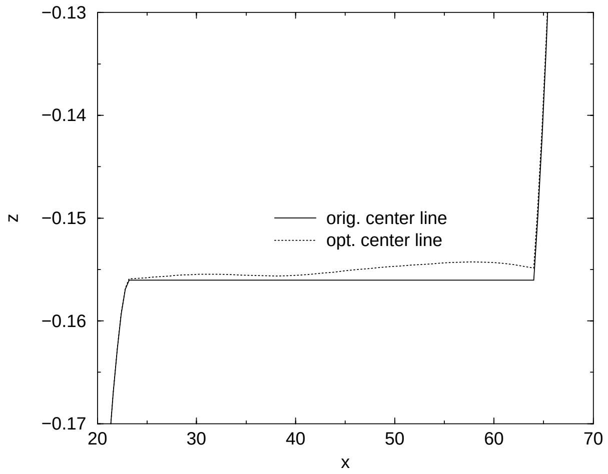

Fig. 9 SCT body centre line for the original and adjoint optimised configuration.

This is due to the fact that the accuracy of the adjoint gradient with respect to these variables is rather poor. These terms are however small, compared to the gradients with respect to the other design variables, and do not influence the over all optimisation convergence.

The radial distribution of the original and optimised body is plotted in figure 8. The body radius is change only locally near the wing and the modified radius deviates less than 2% from the original one. The centre line of the body is also slightly modified (see figure 9).

The optimized wing is slightly twisted up at the root section, to maintain the lift, while in the tip region the wing is twisted down in order to improve the flow attachment and hence reduce the drag. The original and optimized wing at span station $y/b = 0.24, 0.49, 0.70$ and $y/b = 0.92$ are plotted in figures 10,11,12 and 13.

As a final optimisation step the wing thickness was reduced by scaling the wing in such a way that the wing thickness constraint was fulfilled with equality. The thickness for the original and optimisation wing as well as the constraint are plotted in figure 14. An substantial reduction of the drag, due to the reduced wing thickness, was obtained. The lift constrain was fulfilled by slightly modifying the angle of attack from 3.24^o to 3.22^o.

For the complete optimization procedure a total drag reduction from 0.00993 to 0.00837 was obtained which means 15.7%.

The Mach number distribution over the original and optimised aircraft can be seen in figure 19 and the section pressure distribution in the span wise direction, at four wing span stations, are plotted in figure 15,16,17 and 18. We observe that the leading edge pressure peak is reduced

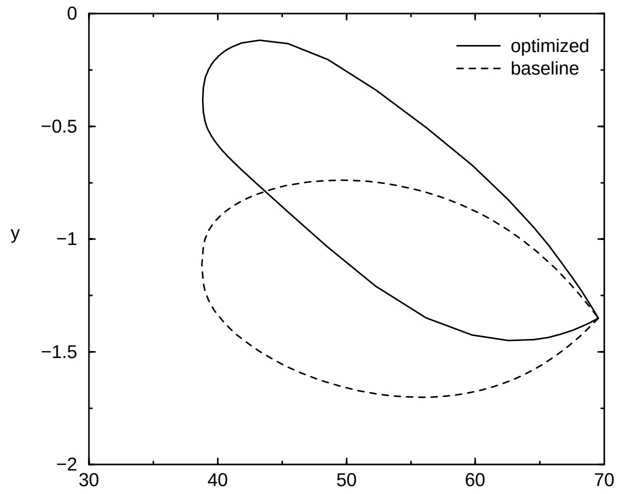

Fig. 10 Wing profiles, in the span wise direction, at span station y/b=0.24 of the original and optimized SCT wing body geometry.

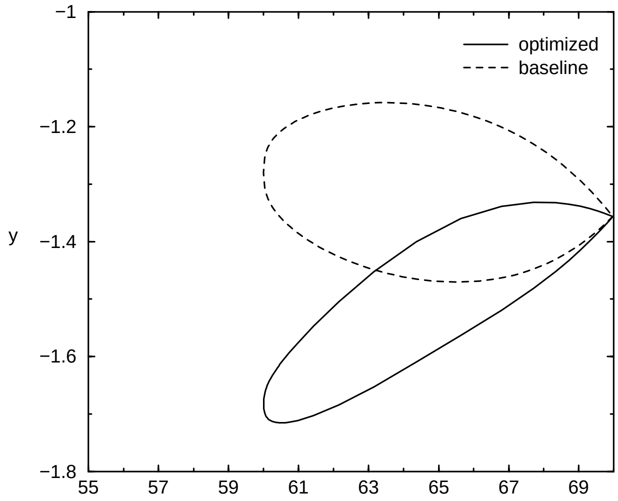

Fig. 12 Wing profiles, in the span wise direction, at span station y/b=0.70 of the original and optimised SCT wing body geometry.

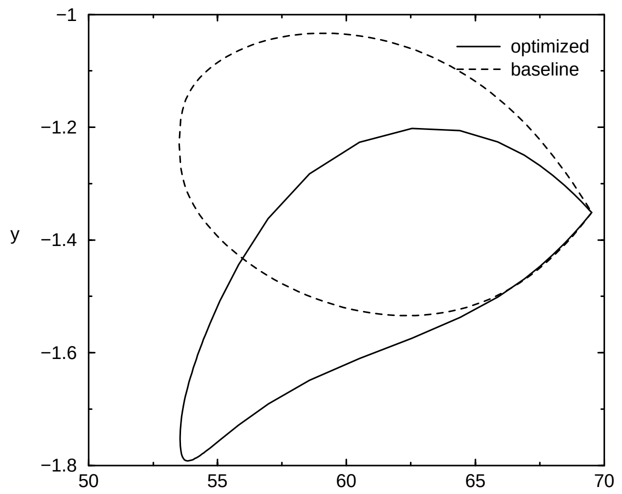

Fig. 11 Wing profiles, in the span wise direction, at span station y/b=0.49 of the original and optimised SCT wing body geometry.

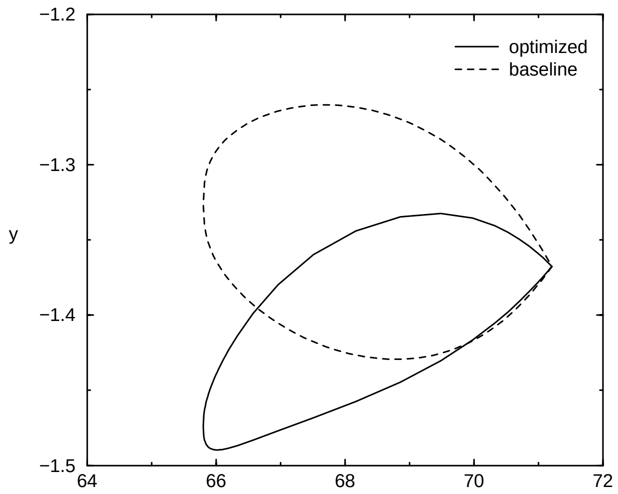

Fig. 13 Wing profiles, in the span wise direction, at span station y/b=0.92 of the original and optimised SCT wing body geometry.

in particular at the middle and outer part of the wing. This yileds a better loading of the wing.

Finally, concerning the computational efficiency one flow and two adjoint calculations is needed in each design step, using the adjoint technique, while the finite difference technique requires 63 flow calculations. This means a ratio of 21, in total computing time, between the two approaches.

7 Summary and Conclusion

The optimisation system **cadsos**, which can handle aerodynamic multi-point designs under multi-constraints, has been applied to the optimisation

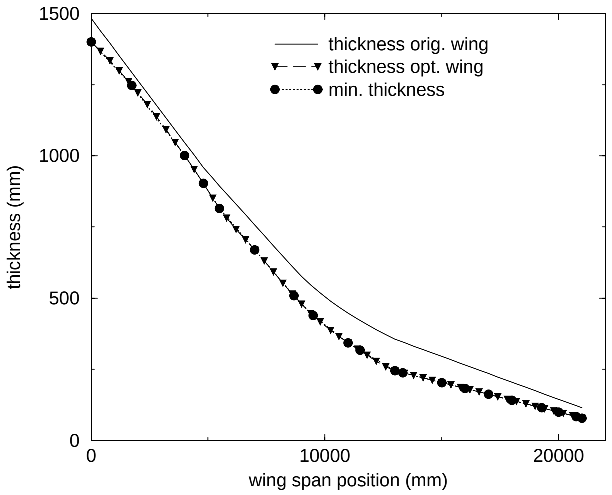

Fig. 14 Thickness distribution of the original and optimized wing.

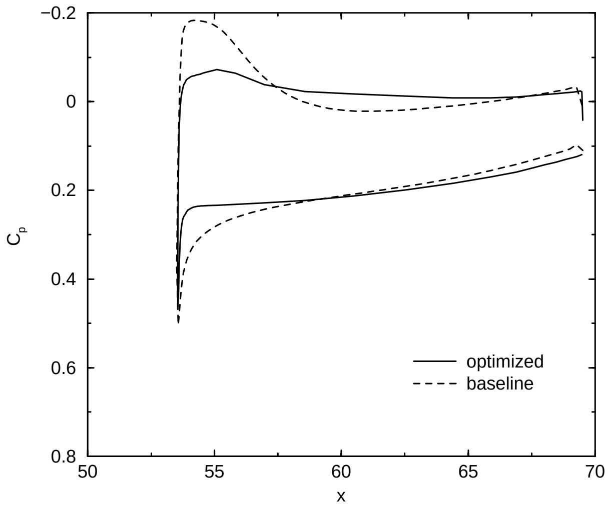

Fig. 16 Wing profiles, in the span wise direction, at span station y/b=0.49 of the original and optimised SCT wing body geometry.

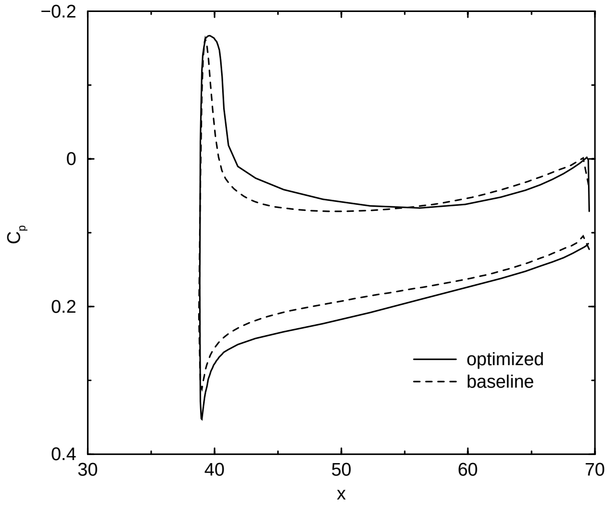

Fig. 15 Pressure distribution in the span wise direction, at span station y/b=0.24 of the original and optimised SCT wing body geometry.

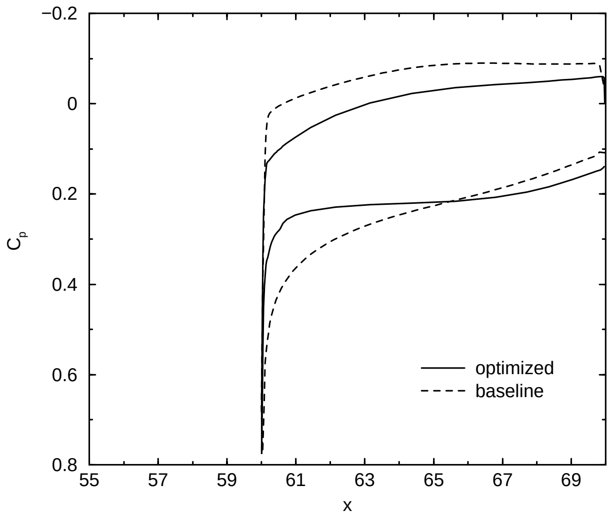

Fig. 17 Wing profiles, in the span wise direction, at span station y/b=.70 of the original and optimised SCT wing body geometry.

of an SCT wing body geometry. An adjoint based gradient technique, in which the gradients are formulated as surface integrals, has been applied. The adjoint optimisation has been compared with finite difference optimization using 62 design variables. A good agreement between adjoint based gradients and finite difference gradients was obtained. It is however important to use high quality grids when computing adjoint based gradients in particular when a surface integral formulation is applied. The two optimisation methods also exhibit the same convergence behavior during a complete optimisation run. The

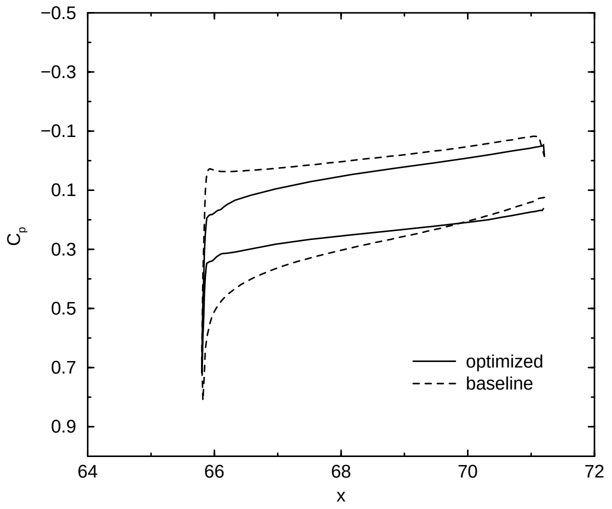

Fig. 18 Wing profiles, in the span wise direction, at span station y/b=0.92 of the original and optimised SCT wing body geometry.

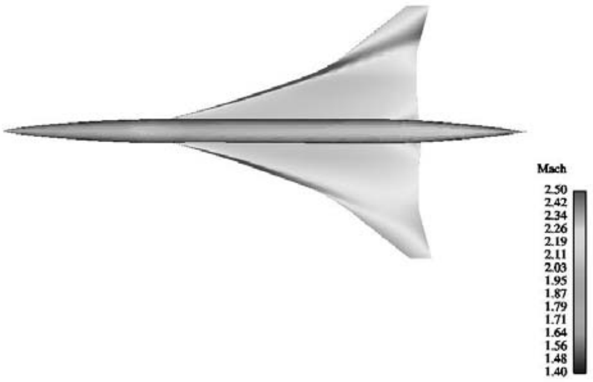

Fig. 19 Mach number distribution on the upper surface of the original (top) and adjoint optimized (bottom) SCT geometry.

adjoint technique is however for more computationally efficient than the finite difference technique. In the present applications a reduction of the computational work with more than a factor of 20 has been achieved.

References

[1] *Criteria for Aerodynamic Design, EUROSUP Tasks 3 and 4 Report, EUROSUP/BAE/T-001*.

[2] Enoksson O and Weinerfelt P. Numerical methods for aerodynamic optimisation. *In proceedings at the 8:th International Symposium on Comp. Fluid Dynamics, Sep. 5-10, 1999, Bremen, Germany*.

[3] Gauger N and Wienberg T. *DLR's contribution to the AEROSHAPE 1st Year Progress Report, AEROSHAPE Deliverable D1-6, Section on Test Case T1.2-1*, 2000.

[4] Gauger N and Wienberg T. *AEROSHAPE Deliverable D1-6, Section on Test Case T1.2-1*, 2001.

[5] Weinerfelt P. Gradient formulations for aerodynamic shape optimisation based on the euler equations. *AEROSHAPE report 2 task3.2 by SAAB*, 2001.

[6] Weinerfelt P. Gradient formulations for aerodynamic shape optimisation based on the navier-stokes equations. *AEROSHAPE report 4 task3.2 by SAAB*, 2001.

Acknowledgement

The present work was funded by the European Union under the contract G4RD-CT1999-00062 entitled AEROSHAPE: Multi Point Aerodynamic Shape Optimisation.